Journal of Molecular Structure 1247 (2022) 131229

Contents lists available at ScienceDirect

Journal of Molecular Structure

journal homepage: www.elsevier.com/locate/molstr

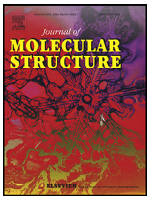

Blue fluorescence from pyridinyl coumarincarboxymides structure having high quantum yield in solution

Zichun Zhou, Xue Tang, Yanhong Cui, Shuai Xue, Zihua Yu, Yujin Li*

College of Chemical Engineering, Zhejiang University of Technology, Hangzhou 310014, People's Republic of China

ARTICLE INFO

Article history:
Received 31 March 2021
Revised 15 July 2021
Accepted 30 July 2021
Available online 2 August 2021

Keywords:
Pyridinecarboxamide
Coumarin
Blue fluorescence
High quantum yield
TD-DFT calculations

ABSTRACT

Small molecules having fluorescence quantum yields are required to promote biological and organic material applications. In this work, we introduced a series of pyridinyl coumarincarboxymides derivatives, namely **4-XP**. These compounds exhibited intense blue fluorescence with high fluorescence quantum yield. By spectral measurement and analysis, it is identified that these pyridine-coumarin conjugates displayed high fluorescence quantum yields ($\Phi_F = 0.77–0.82$) blue fluorescence at about 455 nm in nonpolar solvents. Additionally, the solvent effect and fluorescence properties were verified and explained by DFT and TD-DFT calculations.

1. Introduction

The fluorescent small molecule dyes that have been reported to be used have relatively low fluorescence quantum yield, which limits their application. Therefore, there is an urgent need to develop new small molecule organic fluorescent dyes with high fluorescence quantum yield. Coumarin is an important small fluorophore because of their excellent photophysical properties such as large Stokes shift, high molar absorption coefficient and high quantum yield etc [1,2]. Accordingly, coumarin derivatives are widely used in science and technology, such as perfume, cosmetic, as a disperse dye [3], biocompatible fluorescence dyes [4], charge-transfer agent, solar energy collectors, organic light-emitting diodes (OLEDs) [5], anti-counterfeiting applications [6] etc [7–9]. Therefore, the development of easily synthesizable coumarin fluorescent dyes are highly desirable for practical purposes [10–12].

Coumarin fluorophore can be able to enhance the fluorescence performance based on the intramolecular charge transfer process (ICT) due to the substitution in 7-position and 3-position [13]. For example, Hu's group reported that they prepared coumarin conjugate to employ the intramolecular charge transfer (ICT) to produce quantum yield ($\Phi_F = 0.68$) in toluene and the coumarin conjugate was used as an effective fluorescence water probe in organic solvents [14]. Sekar reported a deep red emitting triphenylamine based coumarin-rhodamine hybrids dyes with large Stokes shift and viscosity sensing [15]. Kaya reported a new coumarin-triazole-based dye with a mirror image and significantly highly of the quantum yields(up to 0.68) [16]. Recently, we developed a fluorescent dyes based on 3-imidazolyl coumarin with unusual solution and solid dual efficient luminescence in high quantum yield ($\Phi_F = 0.90–0.94$ in $CHCl_3$) [17]. Nonetheless, most coumarin fluorescent dyes show green fluorescence, and there are relatively few reports on blue fluorescence of coumarin dyes. Four blue emitting coumarin amide derivatives have been synthesized by Wu and recognized cyanide anion [18]. 7-Diethylaminocoumarin amide compounds exhibited intense blue fluorescence and high fluorescence quantum yields in THF (0.43) [19]. Recently, pyridine moiety is considered as the orientation of heteroaromatic ring aligning toward the donor component can serve as structural tuning factors to modulate the degree of intramolecular charge transfer (ICT) [20,21]. A few literatures have been reported wherein fluorescent dyes of 7-diethylaminocoumarin amide compounds with pyridinyl terminal group. Previous reports suggested that the introduction of pyridine substituent on the fluorescent molecules could serve as an interesting strategy for tuning the photophysical properties [22,23]. The development of blue fluorescent dyes, especially with high fluorescence quantum yield, is the focus of research [24,25]. Herein, a series of pyridinyl coumarincarboxymides based on coumarin derivatives were synthesized and the optical properties were investigated. The coumarin derivatives emitted intense blue fluorescence in different solvents with high quantum yields.

---

* Corresponding author.
E-mail address: lyjzjut@zjut.edu.cn (Y. Li).

https://doi.org/10.1016/j.molstruc.2021.131229
0022-2860/

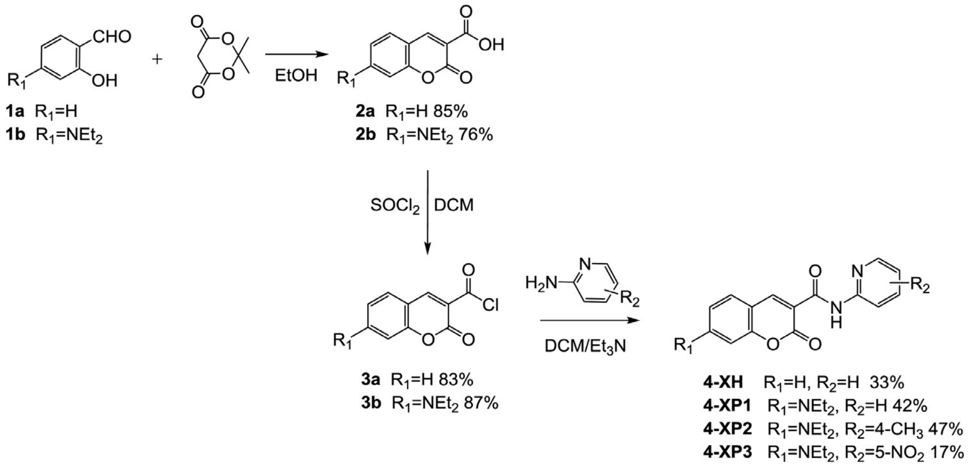

Scheme 1. Synthesis of coumarin derivatives 4.

Table 1
Optical data of **4-XP1** determined in different solvents at room temperature.

Dye	Solvent	λ_{abs}[a] (nm)	ε_{max}[b] ($M^{-1}\cdot cm^{-1}$)	λ_{em}[c] (nm)	Φ_F[d]	SS[e] (nm)
4-XP1	Toluene	424	42,900	446	0.79	22
	DCM	432	47,300	463	0.80	31
	$CHCl_3$	431	51,000	454	0.82	26
	EA	423	46,400	459	0.77	36
	THF	423	44,700	461	0.77	38
	MeCN	428	47,500	473	0.19	45
	DMF	433	48,100	478	0.16	45
	DMSO	435	44,500	483	0.17	48
	EtOH	429	50,500	474	0.21	45
	MeOH	432	47,500	476	0.11	44

Note: [a] All of the values correspond to the strongest absorption peaks.
[b] Molar absorption coefficient.
[c] Emission wavelength.
[d] Fluorescence quantum yields (Φ_F) are measured using an integrating sphere method and standard errors are less than 5%.
[e] The Stokes shift of the experimental results.

2. Results and discussion

2.1. Synthesis

Preparation route of target molecules coumarin derivatives **4** were shown in Scheme 1. Precursors 3-carboxycoumarin **2** were prepared by the reaction of salicylaldehyde derivatives with meldrum's acid in refluxing ethanol solution, which resulted in 85% (R_1 = H) and 76% (R_1 = NEt_2) yields. Then, with the acyl chloride reaction of thionyl chloride, the 3-carboxycoumarin **2** converted to 3-acyl chloride coumarin **3** in 83% (R_1 = H) and 87% (R_1 = NEt_2) yields. The target amide coumarin derivatives were produced by using the amide reaction of 3-acyl chloride coumarin **3** and 2-aminopyridine derivatives under Et_3N condition, which were yielded in 17% to 47%, respectively. The structures of coumarin derivatives **4** were characterized by ^1H NMR, ^{13}C NMR and HR-MS analysis.

2.2. UV–vis absorption and fluorescence emission spectra

2.2.1. The solvent selection of 4-XP1

4-XP1 showed strong fluorescence intensity and obvious solvent effect, so **4-XP1** was chosen for solvent analysis. The absorption and emission spectra of compound **4-XP1** in different solvents were detected and the results were shown in Table 1 and Fig. 1. Compound **4-XP1** exhibited the sharp absorption peak in various organic solvents. Moreover, the solvent had slightly effect on the maximum absorption wavelength (about 430 nm) and the molar absorption coefficient (4.5×10^4 $M^{-1}\cdot cm^{-1}$), and the color of **4-XP1** in different solution appeared as pale yellow under visible light (Fig. 2). Different from the absorption spectrum of **4-XP1**, it was obvious that the intensity of the fluorescence emission peaks and the fluorescence quantum yields (Φ_F) were also greatly affected by the solvents. **4-XP1** showed a strong fluorescence with the similar emission wavelengths ranged from 446 to 476 nm in organic solvents (Table 1), which exhibited the blue fluorescence with high fluorescence quantum yield. As shown in Fig. 1(b), the intensity of the fluorescence emission peaks in non-polar solvents were about 10 times in polar solvents. The emission wavelength of compound **4-XP1** in non-polar solvents were about 460 nm and the corresponding Φ_F were higher than 0.77, such as DCM (0.80), toluene (0.79), THF (0.77), and EA (0.77). Relatively, the Φ_F were sharply reduced in the polar solvents such as MeCN (0.19), DMF (0.16), DMSO (0.17), ethanol (0.21) and methanol (0.11), with a slight red shift of the emission wavelengths around 10–20 nm. This can be explained by the fact that the molecule of **4-XP1** was more stable in the excited state in the polar solvents, which induced non-radiative energy increased and then lead to a red shift of the emission wavelengths [26]. It is noteworthy that the emission wavelength underwent the slight red shift with the increase of solvent polarity and **4-XP1** produced a bright blue fluorescence at 446 nm with $\Phi_F = 0.77$ in toluene. Additionally, in $CHCl_3$, the Φ_F of **4-XP1** was the highest (0.82) and the emission peak of **4-XP1** was found at 454 nm. Furthermore, although the Φ_F of **4-XP1** was lower in the polar solvents, but it had larger Stokes shift (44–48 nm) than that in the non-polar solvents (22–38 nm).

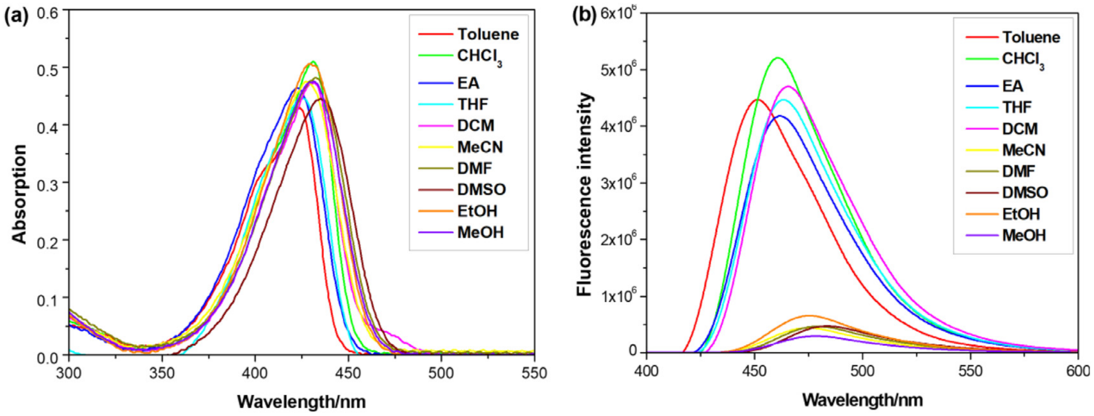

Fig. 1. (a) UV–Vis absorption spectra and (b) fluorescence spectra of **4-XP1** in different solvents (For interpretation of the references to color in this figure, the reader is referred to the web version of this article.).

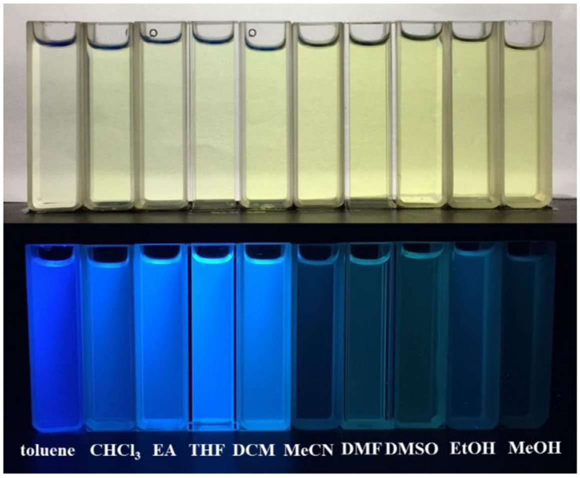

Fig. 2. The color of **4-XP1** (left to right: toluene, CHCl$_3$, EA, THF, DCM, MeCN, DMF, DMSO, EtOH, MeOH) under the visible light (upper row) and the UV lamp (365 nm, lower row) (For interpretation of the references to color in this figure, the reader is referred to the web version of this article.).

Table 2
Optical data of compound 4 in CHCl$_3$.

Dye	λ_{abs}^{a} (nm)	ε_{max}^{b} ($M^{-1}\cdot cm^{-1}$)	λ_{em}^{c} (nm)	Φ_F^{d}	SS^e (nm)
4-XH	307	13,900	375	0.03	68
4-XP1	431	51,000	454	0.82	26
4-XP2	431	34,800	457	0.85	23
4-XP3	444	54,500	467	0.12	23

Note: [a] All of the values correspond to the strongest absorption peaks.
[b] Molar absorption coefficient.
[c] Emission wavelength.
[d] Fluorescence quantum yields (Φ_F) are measured using an integrating sphere method and standard errors are less than 5%.
[e] The Stokes shift of the experimental results.

2.2.2. Optical properties of compound *4* in CHCl$_3$

According to the spectral performance of compound **4-XP1** in different solvents, the UV–Vis absorption and fluorescence emission spectrum of compound **4** (**4-XH**, **4-XP2** and **4-XP3**) were measured in CHCl$_3$ and the results were shown in Table 2 and Fig. 3. Compound **4-XH** showed an absorption peak at 307 and 347 nm and its molar absorption coefficient (ε) was 1.4×10^4 $M^{-1}\cdot cm^{-1}$. In the structure of **4-XH**, the charge was concentrated in the pyridine ring, and a strong intramolecular charge transfer (ICT) occurred during the excitation process, so an ICT peak (347 nm) was generated. The corresponded fluorescence emission peak of **4-XH** was at around 375 nm with a weak fluorescence intensity ($\Phi_F = 0.03$). It is obvious that the solution color of **4-HX** displayed colorless with fluorescence quenching (Fig. 4). It can be seen from the results that **4-XP1**, **4-XP2** and **4-XP3** had similar absorption peaks at about 431 nm and the blue fluorescence emission wavelength at about 460 nm. It is worth mentioning that **4-XP3** showed another absorption peak at 315 nm due to the π-π transition. On moving from **4-XP1** to **4-XP2** and **4-XP3**, the fluorescence emission peak was slightly redshifted from 455 to 467 nm. Meanwhile, **4-XP1** and **4-XP2** exhibited intense blue fluorescence and high fluorescence quantum yields (**4-XP1**: 0.82, **4-XP2**: 0.85) in CHCl$_3$. It is worth noting that the absorption and fluorescence emission peaks of compounds **4-XP** (diethylamino substituted in 7-position) were redshifted obviously and intensity increased dramatically compared with **4-XH** (H in 7-position), which indicated that the introduction of the diethylamine group in coumarin 7-position was benefit to the absorption and fluorescence properties of the compounds. In comparison, due to the introduction of the nitro group in pyridine 5-position, **4-XP3** exhibited the highest molar absorption coefficient ($\varepsilon = 5.5 \times 10^4$ $M^{-1}\cdot cm^{-1}$) and the lowest fluorescence quantum yield ($\Phi_F = 0.12$) relative to that of **4-XP1** and **4-XP2** in CHCl$_3$. Although the molar absorption coefficient and Φ_F of **4-XP1**, **4-XP2** and **4-XP3** were higher than **4-XH** in CHCl$_3$, the introduction of diethylamino group reduced the corresponded Stokes shift (68 nm) to the ranged of 23–26 nm. As clearly seen from Fig. 4., **4-XP1** and **4-XP2** appeared as pale-yellow color under visible light and intense blue fluorescence under UV radiation in CHCl$_3$, yet **4-XP3** displayed dark yellow color and were shown as weak blue fluorescence.

2.3. Theoretical calculation

To better understand the optical properties of the fluorescent molecule **4**, DFT and TD-DFT calculations were applied to our research [27–32]. The geometrical configuration of the compound **4-XP1** was optimized by applying the DFT to obtain the optimal structure at the B3LYP/6–311 G level of theory, as implemented in the Gaussian 09 program package (Fig. 5) [33]. Further, we had calculated the absorption and emission spectra by using polarizable continuum model (PCM) in different solvents at the B3LYP/6–311 G level. By using the DFT calculations, the orbital energies of LUMO and HOMO were calculated, and then the absorption and emission spectra were computed by using TD-DFT (Table 3).

In order to determine the stable structure of **4-XP1**, the ground state energies of enol and keto configuration of amide structure were calculated in different solvents and the energy of keto form was lower than enol form. Therefore, the stable structure of **4-XP1**

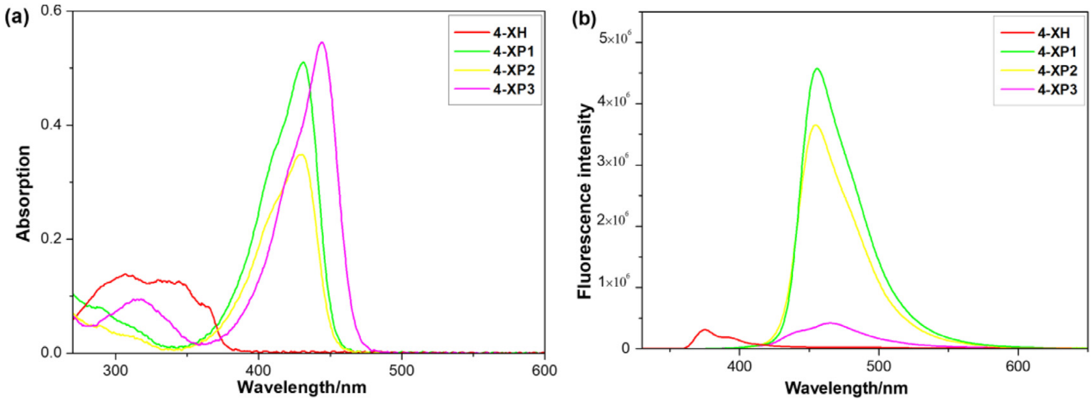

Fig. 3. (a) UV–Vis absorption spectra and (b) fluorescence spectra of compounds **4** in $CHCl_3$.

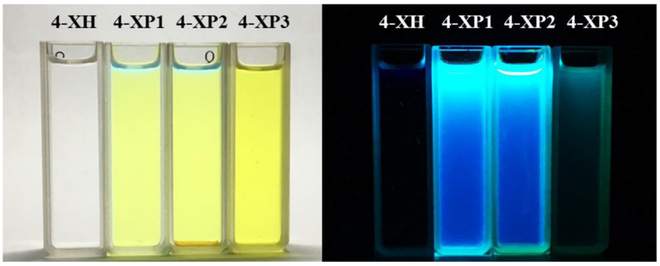

Fig. 4. The color of compound **4** in $CHCl_3$ under the visible light and the UV lamp (365 nm) (For interpretation of the references to color in this figure, the reader is referred to the web version of this article.).

was stable in keto form and the stable geometry in $CHCl_3$ was shown in Fig. 5. In the molecular structure of **4-XP1**, coumarin and amide are in plane structure through hydrogen bond between carbonyl group on coumarin ring and hydrogen of amide, while pyridine ring has a certain dihedral angle with coumarin plane through C-N bond rotation.

The optimized ground state and excited state configurations in different solvents were shown in Fig. 6 and it can be seen that the pyridine ring of **4-XP1** (the single bond between C19 and N18) rotates in the excited state. In non-polar solvent, the rotation angles were 23.70° (toluene) and 23.95° ($CHCl_3$), respectively, but it increased to 37.59° in DMSO and 37.31° in methanol. The increase of rotation angle leaded to the increase of nonradiative energy, which may be the cause of the decrease of fluorescence intensity, the red shift of absorption and emission wavelength and the increase of Stokes shift of **4-XP1** in polar solvents. There were in good agreement with the experimental results.

Based on the optimized structure, the absorption and emission spectra of **4-XP1** in five different solvents (toluene, $CHCl_3$, tetrahydrofuran, dimethyl sulfoxide and methanol) were calculated by TD-DFT (Table 3 and Fig. 7). As shown in Table 3, the absorption and emission wavelengths of **4-XP1** were increased with the increase of solvent polarity, which was consistent with the experimental results. As shown in Fig. 7, the LUMO energy levels were -2.63 and -2.64 eV in the nonpolar solvents chloroform and THF, while in the polar solvent DMSO, the LUMO energy levels dropped to -2.67 eV. The energy gap also decreased with the increase of solvent polarity, from 3.50 eV (toluene) to 3.21 eV (DMSO), and the emission wavelength was red shifted.

We also calculated the optical properties of compound **4** based on the structure optimization. In order to further verify the experimental results, the geometry of compound **4** was optimized by DFT calculation at the B3LYP / 6–311+G (d) level through the polarization continuum model (PCM) in $CHCl_3$. Based on the optimized structure, the frontier orbital energy of compound **4** was calculated by time-dependent density functional theory (TD-DFT), and then the absorption and emission spectra were calculated (Table 4 and Fig. 8).

From the frontier molecular orbitals and transition energies of compound **4** (Fig. 8 and Table 4), it can be seen that the transition mode of **4-XP** was from HOMO to LUMO, while that of **4-XH** was from HOMO-3 to LUMO. The electron cloud of **4-XH** was mainly concentrated on the pyridine ring in the ground state (HOMO), while in excited state was mainly concentrated on the coumarin ring (LUMO). During the excitation process, intramolecular charge transfer (ICT) led to the increase of non-radiative energy, resulting in lower fluorescence intensity and larger Stokes shift [34,35]. Pyridine as a key contributing part of the designed dyes. The introduction of pyridine ring increased the conjugation system of **4-XP1** and **4-XP2** and the electron delocalization, which resulted the electron cloud of HOMO and LUMO orbitals evenly distributed in the whole molecule. This may be one of the factors affecting the higher fluorescence intensity. At the same time, we also noticed that the HOMO electron cloud of **4-XP3** is concentrated on the coumarin ring, while the LUMO electron cloud is concentrated on the pyridine ring, similar to **4-XH**, resulting in the decrease of fluorescence intensity, which was consistent with the experimental results. It can be seen from Fig. 8 that the possible reason is that the introduction of the electron withdrawing group (nitro group) and the electron donor group (diethylamino

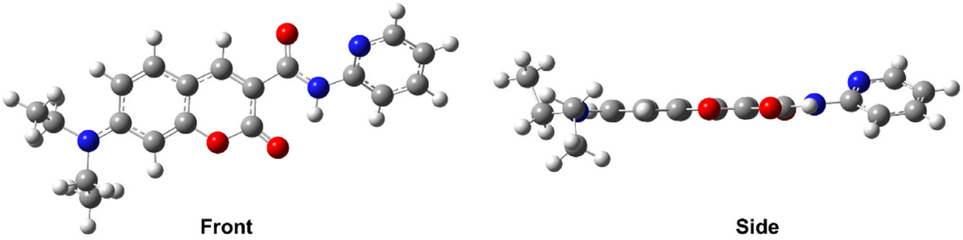

Fig. 5. Optimized geometry of **4-XP1** at B3LYP/6–311 G level.

Table 3
Calculation data of compounds **4-XP1** in differrent solvents at B3LYP/6–311 G level.

Solvent	$\lambda_{cal}{}^{a}$ (nm) / f ^{e}	$\lambda_{abs}{}^{b}$ (nm)	$\lambda_{cal}{}^{c}$ (nm) / f ^{e}	$\lambda_{em}{}^{d}$ (nm)	Energy gap (eV)
Toluene	390 / 1.0192	424	412 / 0.9638	446	3.50
$CHCl_3$	403 / 1.1023	431	426 / 1.0827	454	3.27
THF	409 / 1.1370	423	432 / 1.1122	461	3.25
DMSO	419 / 1.1927	435	443 / 1.1696	483	3.21
MeOH	419 / 1.1880	432	442 / 1.1651	476	3.22

Note: [a]The calculated maximum absorption wavelength.
[b] The experimental maximum absorption wavelength.
[c] The calculated maximum emission wavelength.
[d] The experimental maximum emission wavelength.
[e] Oscillator strength coefficients.

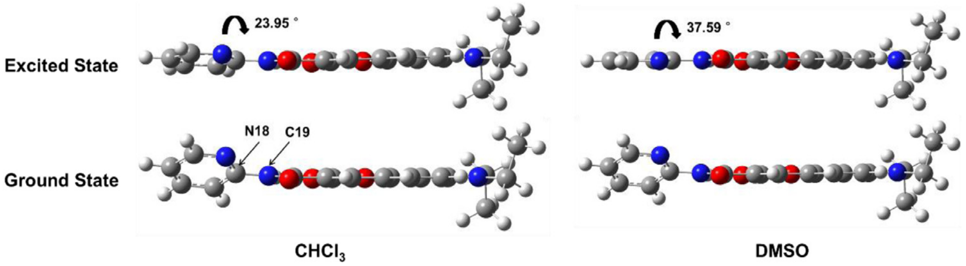

Fig. 6. Ground state and excited state configuration of compound **4-XP1** in $CHCl_3$ and DMSO.

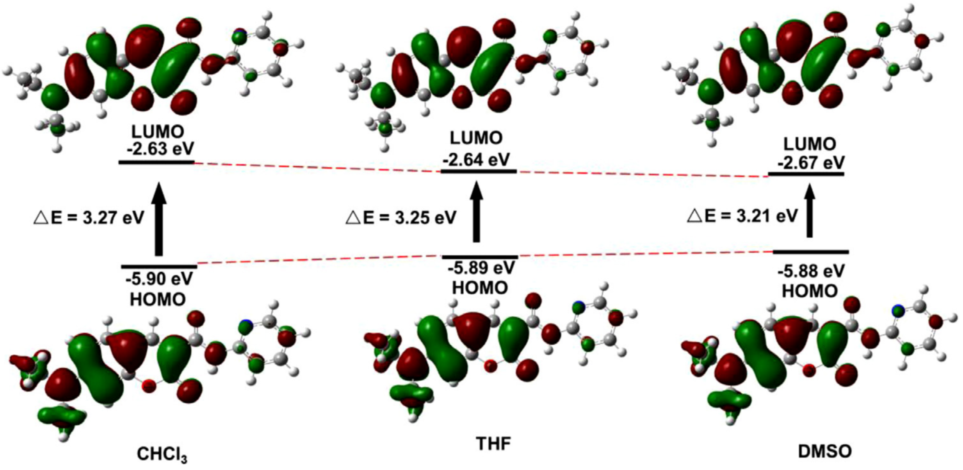

Fig. 7. Frontier molecular orbitals of **4-XP1** in $CHCl_3$, THF and DMSO.

Table 4
Calculation data of compounds **4** in differrent solvents at B3LYP/6–311+G(d) level.

Dye	$\lambda_{cal}{}^{a}$ (nm) / f ^{e}	$\lambda_{abs}{}^{b}$ (nm)	$\lambda_{cal}{}^{c}$ (nm) / f ^{e}	$\lambda_{em}{}^{d}$ (nm)	Energy gap (eV)
4-XH	303 / 0.3337	307	386 / 0.2672	375	4.13
4-XP1	401 / 1.1336	431	425 / 1.1481	454	3.32
4-XP2	401/ 1.1403	431	426 / 1.1690	457	3.31
4-XP3	476 / 0.4665	444	632 / 0.1872	467	2.25

Note: [a]The calculated maximum absorption wavelength.
[b] The experimental maximum absorption wavelength.
[c] The calculated maximum emission wavelength.
[d] The experimental maximum emission wavelength.
[e] Oscillator strength coefficients.

group) at the 7 position of the coumarin in the **4-XP3** molecule formed a push-pull effect, which significantly changed the electron cloud distribution of **4-XP1** resulting a very small energy gap (2.25 eV), which caused a red shift of the absorption and emission wavelengths.

From the specific spectral data in Table 4, the maximum absorption wavelength of **4-XH** was at 303 nm and the maximum absorption wavelengths of **4-XP** were red shifted 98–173 nm due to the introduction of diethylamino group. The emission wavelengths of **4-XP1** and **4-XP2** were red shifted from 386 nm (**4-XH**) to about 425 nm. The theoretical calculated data have the same trend with the experimental values. The energy gap of **4-XH** was 4.13 eV, while the other three compounds were relatively small (2.25–3.32 eV), so it was easier to transition than **4-XH**. The calculation results of TD-DFT verified the reason that the fluorescence of **4-XP** was stronger in the experimental results.

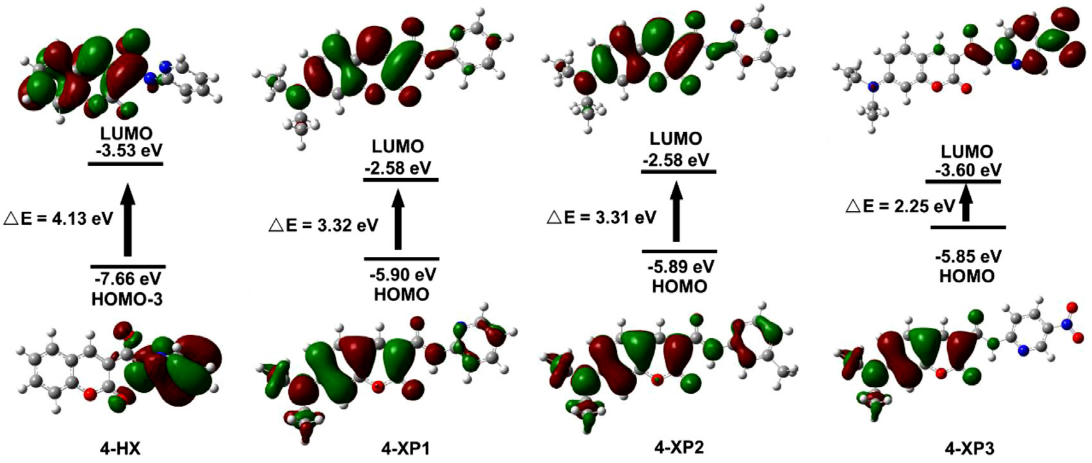

Fig. 8. Frontier molecular orbitals of compounds **4** in $CHCl_3$ at B3LYP/6–311+G(d) level.

3. Conclusion

In conclusion, a series of pyridinecarboxamides based on coumarin derivatives were designed and synthesized. These dyes exhibited the blue fluorescence with high quantum yields in nonpolar solvents. Moreover, the emission wavelength underwent a red shift and the fluorescence quantum yields were significantly reduced in polar solvent. Such solvent-sensitive fluorescent dyes provide experimental reference data for the research of microenvironment-sensitive fluorescent probes. We also found that compound **4-XP3** with nitro substituted on the pyridyl ring reduced fluorescence intensity and underwent a red shift of absorption/emission wavelength. The electron donating group linked on the pyridine ring has little effect on the fluorescence performance, but the linking electron withdrawing group significantly changes the fluorescence performance. This type of dyes can be used for different applications by modifying the substituents. Besides, the absorption and emission spectra of compounds **4** in different solvents were calculated by DFT calculations agreed with the experimental spectra. The results showed that pyridinecarboxamides based on coumarin derivatives displayed attractive and tunable luminescent properties which can be applied in blue fluorescent dyes, fluorescent sensor and biological imaging.

4. Experimental

4.1. Materials and equipment

All of the chemicals used in the current study were purchased from commercial vendors and used as received without further purification, unless otherwise noted. All solvents were purified and dried using standard methods prior to use. Nuclear magnetic resonance (^1H, ^{13}C) spectra were recorded on a Bruker AM 500 spectrometer with chemical shifts reported as ppm at 500, 125 MHz, respectively, (in DMSO, $CDCl_3$ and TMS as the internal standard). The high-resolution mass spectra were recorded on a Thermo Scientific LTQ Orbitrap XL (ESI) and melting points (Mp.) were recorded on a X-4 electro-thermal digital melting point apparatus.

4.2. Absorbance, fluorescence and quantum yield

The solvents used in the photochemical measurements were spectroscopic grade. All the experiments were performed repeatedly, and reproducible results were obtained. UV–Vis absorption spectra were measured on a UV-2550. Fluorescence spectra were obtained with an Edinburgh FS5 spectrofluorometer. The Φ_F values in solution were measured using an integrating sphere method and dilute solutions of the compounds in organic solvent were used (1×10^{-5} mol/L). The fluorescence spectra were recorded 3 times.

4.3. General procedure for the synthesis of compounds

*4.3.1. General preparation of compounds 3-carboxycoumarin derivatives **2***

A mixture of salicylaldehyde 1a (10.0 mmol, 1.210 g), meldrum's acid (10.0 mmol, 1.441 g) in ethanol (10 mL) was stirred to reflux for 12 h. The reaction was complete detected by TLC and cooled to room temperature, and then the reaction precipitate was filtered to give crude product. The crude product was purified by recrystallized from anhydrous ethanol solvent (5 mL) to afford target compound **2a** (1.616 g, 85%) as white solid without further purification. The synthesis process of **2b** was similar to **2a**.

*4.3.2. General preparation of compounds 3-acyl chloride coumarin derivatives **3***

A mixture of 3-carboxycoumarin **2a** (10.0 mmol, 1.901 g), anhydrous thionyl chloride (4 mL) and anhydrous DMF (0.1 mL) was stirred at room temperature for 1 h. The reaction was complete detected by TLC and the solvent was removed under reduced pressure to afford target compound **3a** (1.447 g, 83%) as white solid. The synthesis process of **3b** was similar to **3a**.

*4.3.3. General preparation of compounds 3-carboxamide coumarin derivatives **4***

3-Acyl chloride coumarin **3a** (0.416 g, 2.0 mmol), Et_3N (2.021 g, 20.0 mmol), 2-aminopyridine (0.188 g, 2.0 mmol) and DCM (10 mL) were added in turn to a 50 mL round-bottomed flask. The reaction was stirred for 12 h at room temperature and completed the reaction was detected by TLC analysis. The mixture was washed with water (20 mL) and extracted with dichloromethane (3×30 mL). The organic layer was combinated and dried with Na_2SO_4, and then removed the solvent under reduced pressure. The residue was purified by silica gel chromatography eluting (silica gel, petroleum ether/ethyl acetate = 2:1) to afford complex **4-XH** (0.177 g, 33%) as a white solid. The synthesis process of **4-XP1**∼**4-XP3** was similar to **4-XH**.

*4.3.4. 2-oxo-N-(pyridin-2-yl)-2H-chromene-3-carboxamide (compound **4-XH**)*

White solid. Yield 33%. Mp. 252–254 °C. ^1H NMR (500 MHz, DMSO-d_6) δ (ppm): 11.17 (s, 1H), 9.07 (s, 1H), 8.39 (d, J = 3.9 Hz, 1H), 8.28 (d, J = 8.3 Hz, 1H), 8.07 (d, J = 6.9 Hz, 1H), 7.90

(t, J = 7.0 Hz, 1H), 7.82 (t, J = 7.8 Hz, 1H), 7.57 (d, J = 8.4 Hz, 1H), 7.50 (t, J = 7.4 Hz, 1H), 7.27–7.16 (m, 1H). ^{13}C NMR (125 MHz, DMSO-d$_6$) δ (ppm): 161.45 (1C), 160.35 (1C), 154.55 (1C), 151.38 (1C), 149.11 (1C), 148.98 (1C), 139.18 (1C), 135.19 (1C), 131.08 (1C), 125.87 (1C), 120.87 (1C), 119.15 (1C), 119.03 (1C), 116.77 (1C), 114.22 (1C).

*4.3.5. 7-(diethylamino)-2-oxo-N-(pyridin-2-yl)-2H-chromene-3-carboxamide (compound **4-XP1**)*

Yellow solid. Yield 42%. Mp. 255–256 °C. ^{1}H NMR (500 MHz, CDCl$_3$) δ (ppm): 11.32 (s, 1H), 8.76 (s, 1H), 8.36 (d, J = 8.2 Hz, 2H), 7.72 (t, J = 8.7 Hz, 1H), 7.45 (d, J = 9.0 Hz, 1H), 7.09–7.00 (m, 1H), 6.66 (d, J = 9.0 Hz, 1H), 6.52 (s, 1H), 3.46 (q, J = 7.1 Hz, 4H), 1.24 (t, J = 7.1 Hz, 6H). ^{13}C NMR (125 MHz, CDCl$_3$) δ (ppm): 162.52 (1C), 158.02 (1C), 153.00 (1C), 148.69 (2C), 148.29 (1C), 138.04 (1C), 131.42 (2C), 119.64 (1C), 114.68 (1C), 110.14 (2C), 108.58 (1C), 96.75 (1C), 45.20 (2C), 12.44 (2C). HRMS (ESI) *m/z* calcd for $C_{19}H_{20}N_3O_3^+$ (M+H) $^+$ 338.14992, found 338.14975.

*4.3.6. 7-(diethylamino)-N-(4-methylpyridin-2-yl)-2-oxo-2H-chromene-3-carboxamide (compound **4-XP2**)*

Yellow solid. Yield 47%. Mp. 267–268 °C. ^{1}H NMR (500 MHz, CDCl$_3$) δ (ppm): 11.26 (s, 1H), 8.76 (s, 1H), 8.34–8.02 (m, 2H), 7.46 (d, J = 9.0 Hz, 1H), 6.87 (d, J = 4.9 Hz, 1H), 6.66 (d, J = 11.3 Hz, 1H), 6.53 (s, 1H), 3.46 (q, J = 7.1 Hz, 4H), 2.39 (s, 3H), 1.25 (t, J = 7.1 Hz, 6H). ^{13}C NMR (125 MHz, CDCl$_3$) δ (ppm): 162.49 (1C), 161.51 (1C), 157.98 (1C), 152.96 (1C), 151.83 (1C), 149.40 (1C), 148.59 (1C), 147.89 (1C), 131.40 (1C), 120.86 (1C), 115.20 (1C), 110.05 (1C), 109.98 (1C), 108.57 (1C), 96.74 (1C), 45.19 (2C), 21.42 (1C), 12.44 (2C). HRMS (ESI) *m/z* calcd for $C_{20}H_{22}N_3O_3^+$ (M+H) $^+$ 352.16557, found 352.16574.

*4.3.7. 7-(diethylamino)-N-(5-nitropyridin-2-yl)-2-oxo-2H-chromene-3-carboxamide (compound **4-XP3**)*

Orange solid. Yield 17%. Mp. 277–278 °C. ^{1}H NMR (500 MHz, CDCl$_3$) δ (ppm): 11.36 (s, 1H), 8.75 (s, 1H), 8.39 (d, J = 2.2 Hz, 1H), 8.31 (d, J = 8.8 Hz, 1H), 7.80 (dd, J = 8.8, 2.4 Hz, 1H), 7.45 (d, J = 9.0 Hz, 1H), 6.66 (dd, J = 9.0, 2.4 Hz, 1H), 6.52 (d, J = 2.3 Hz, 1H), 3.47 (q, J = 7.1 Hz, 4H), 1.25 (t, J = 7.1 Hz, 6H). ^{13}C NMR (125 MHz, CDCl$_3$) δ (ppm): 162.54 (1C), 161.62 (1C), 158.04 (1C), 153.12 (1C), 150.53 (1C), 149.07 (1C), 148.80 (1C), 140.41 (1C), 131.50 (1C), 115.82 (1C), 114.47 (1C), 110.24 (1C), 109.43 (1C), 108.55 (1C), 96.72 (1C), 45.22 (2C), 12.44 (2C). HRMS (ESI) *m/z* calcd for $C_{19}H_{19}N_4O_5^+$ (M+H) $^+$ 383.13500, found 383.13559.

Declaration of Competing Interest

We declare that we have no financial and personal relationships with other people or organizations that can inappropriately influence our work, there is no professional or other personal interest of any nature or kind in any product, service and/or company that could be construed as influencing the position presented in, or the review of, the manuscript entitled.

CRediT authorship contribution statement

Zichun Zhou: Visualization, Formal analysis, Writing – review & editing. **Xue Tang:** Methodology, Formal analysis, Writing – review & editing. **Yanhong Cui:** Methodology, Formal analysis, Writing – review & editing. **Shuai Xue:** Formal analysis, Writing – review & editing. **Zihua Yu:** Formal analysis, Writing – review & editing. **Yujin Li:** Project administration, Formal analysis, Writing – review & editing.

Acknowledgement

We gratefully acknowledge the financial supported by the Natural Science Foundation of China (21606201) and the National Natural Science Foundation of Zhejiang (LY13B020016) and the Undergraduate Science and Technological Innovation Program in Zhejiang Province (Zhejiang Xinmiao Talents Program) (2017R403066).

Supplementary materials

Supplementary material associated with this article can be found, in the online version, at doi:10.1016/j.molstruc.2021.131229.

References

[1] S.H. Zhou, J.H. Jia, J.R. Gao, L. Han, Y.J. Li, W.J. Sheng, The one-pot synthesis and fluorimetric study of 3-(2′-benzothiazolyl)coumarins, Dyes Pigments 86 (2010) 123–128.

[2] T.Z. Yu, S.D. Yang, Y.L. Zhao, H. Zhang, X.Q. Han, D.W. Fan, Y.Q. Qiu, L.L. Chen, Synthesis, crystal structures and fluorescence properties of 3-(2-pyridyl)coumarin derivatives, J. Photoch. Photobio. A 214 (2010) 92–99.

[3] K.V. Basavarajappa, Y.A. Nayaka, R.O. Yathisha, P. Manjunatha, Synthesis, Characterization, Optical, Electrochemical and Current-Voltage Characteristics of Coumarin Dyes, J. Fluoresc. 29 (2019) 1201–1211.

[4] L. Sun, J. Liu, S. Xu, B. Dong, J. Lv, S. Hu, B. Zhou, B. Shen, Y. Wang, L. Xu, W. Xu, X. Bai, H. Song, High fluorescence LaOBr/coumarin organic–inorganic composite nanomaterials for ultra-sensitive Fe^{3+} sensing, fluorescence imaging and water-based ink anti-counterfeiting applications, J. Mater. Chem. C 8 (2020) 13733–13742.

[5] A. Alizadeh, B. Farajpour, S.S. Mohammadi, M. Sedghi, H. Naderi-Manesh, C. Janiak, T.O. Knedel, Design and Synthesis of Coumarin-Based Pyrazolopyridines as Biocompatible Fluorescence Dyes for Live-Cell Imaging, ChemistrySelect 5 (2020) 9362–9369.

[6] S.A.R. Nurhayatun, J. Joazaizulfazli, C. Subhash, W. Roswanira Abdul, P.B. Deepak, K.S. Terry, S. Murugesan, Coumarin-Oxadiazole Derivatives: Synthesis and Pharmacological Properties, Mini Rev. Org. Chem. 17 (2020) 780–794.

[7] F.J. Chen, G.Z. Liu, Y.J. Shi, P.X. Xi, J. Cheng, J.P. Hong, R. Shen, X.J. Yao, D.C. Bai, Z.Z Zeng, A coumarin-derived fluorescent chemosensor for selectively detecting Cu^{2+}: Synthesis, DFT calculations and cell imaging applications, Talanta 124 (2014) 139–145.

[8] C.J. Hua, K. Zhang, M. Xin, T. Ying, J.R. Gao, J.H. Jia, Y.J. Li, High quantum yield and pH sensitive fluorescence dyes based on coumarin derivatives: fluorescence characteristics and theoretical study, RSC Adv. 6 (2016) 49221–49227.

[9] P. Li, M. Zhang, X. Sun, S. Guan, G. Zhang, M. Baumgarten, K. Mullen, A dendrimer-based highly sensitive and selective fluorescence-quenching sensor for Fe^{3+} both in solution and as film, Biosens. Bioelectron. 85 (2016) 785–791.

[10] N. Ahmed, B.V. Babu, S. Singh, P.M. Mitrasinovic, An Efficient One-Pot Three-Component Synthesis of Highly Functionalized Coumarin Fused Indenodihydropyridine and Chromeno[4,3-b]quinoline Derivatives, Heterocycles 85 (2012) 1629–1653.

[11] A. Thakur, R. Singla, V. Jaitak, An Efficient One-Pot Three-Component Synthesis of Highly Functionalized Coumarin Fused Indenodihydropyridine and Chromeno[4,3-b]quinoline Derivatives, Eur. J. Med. Chem. 101 (2015) 476–495.

[12] C. Fan, X. Huang, L. Han, Z. Lu, Z. Wang, Y. Yi, Novel colorimetric and fluorescent off–on enantiomers with high selectivity for Fe^{3+} imaging in living cells, Sens. Actuators B Chem. 224 (2016) 592–599.

[13] G. Mata, N.W. Luedtke, Synthesis and Solvatochromic Fluorescence of Biaryl Pyrimidine Nucleosides, Org. Lett. 15 (2013) 2462–2465.

[14] K.P. Wang, Y. Lei, J.P. Chen, Z.H. Ge, W. Liu, Q. Zhang, S.J. Chen, Z.Q. Hu, The coumarin conjugate: synthesis, photophysical properties and the ratiometric fluorescence response to water content of organic solvent, Dyes Pigments 151 (2018) 233–237.

[15] K. Shantaram, G.J. Amol, S. Nagaiyan, Deep red emitting triphenylamine based coumarin-rhodamine hybrids with large Stokes shift and viscosity sensing: Synthesis, photophysical properties and DFT studies of their spirocyclic and open forms, Dyes Pigments 137 (2017) 329–341.

[16] M. Kaya, E. Menteşe, Synthesis and solvent-dependent photophysics of a novel fluorescent triazole-coumarin-based dye, J. Heterocycl. Chem. 57 (2020) 1714–1719.

[17] Z.C. Zhou, A.N. Zheng, Y.H. Cui, Z.Q. Lin, W.J. Niu, Y.J. Zhang, J.R. Gao, Y.J. Li, Rational design and synthesis of 3-heteroaromatics coumarin molecules with unusual solution and solid dual efficient luminescence, Tetrahedron 75 (2019) 2958–2964.

[18] Q.Q. Wu, Z.Q. Liu, D.X. Cao, R.F. Guan, K.G. Wang, Y.Y. Shan, Y.G. Xu, L. Ma, Coumarin amide derivatives as fluorescence chemosensors for cyanide anions, Mater. Chem. Phys. 161 (2015) 43–48.

[19] Y.T. Sun, Y.H. Sun, S.F. Zhao, D.X. Cao, R.F. Guan, Z.Q. Liu, X.Y. Yu, X. Zhao, Efficient Solution- and Solid-State Fluorescence for a Series of 7-Diethylaminocoumarin Amide Compounds, Asian J. Org. Chem. 7 (2018) 197–202.

[20] C. Zhang, M. Li, W. Liang, G. Zhang, L. Fan, Q. Yao, S. Shuang, C. Dong, Substituent Effect on the Properties of pH Fluorescence Probes Containing Pyridine Group, ChemistrySelect 4 (2019) 5735–5739.

[21] K.C. Pan, S.W. Li, Y.Y. Ho, Y.J. Shiu, W.L. Tsai, M. Jiao, W.K. Lee, C.C. Wu, C.L. Chung, T. Chatterjee, Y.S. Li, K.T. Wong, H.C. Hu, C.C. Chen, M.T. Lee, Efficient and Tunable Thermally Activated Delayed Fluorescence Emitters Having Orientation-Adjustable CN-Substituted Pyridine and Pyrimidine Acceptor Units, Adv. Funct. Mater. 26 (2016) 7560–7571.

[22] G. Gogoi, D. kashyap, R.J. Sarma, Mechano-Luminescent Behavior of a Pyridine–Containing Anthracene Derivative: Role of Aromatic Stacking Interactions, Cryst. Growth Des. 18 (2018) 4963–4970.

[23] K.N. Indravath, B. Ramakrishna, S. raditya, M. Navendu, K.D. Samar, Functional Molecular System of Bis(pyrazolyl)pyridine Derivatives: Photophysics, Spectroscopy, Computation, and Ion Sensing, ACS Omega 3 (2018) 3022–3035.

[24] C.J. Hua, H. Zheng, K. Zhang, M. Xin, J.R. Gao, Y.J. Li, A novel turn off fluorescent sensor for Fe(III) and pH environment based on coumarin derivatives: the fluorescence characteristics and theoretical study, Tetrahedron 72 (2016) 8365–8372.

[25] Z.C. Zhou, W.J. Niu, Z.Q. Lin, Y.H. Cui, X. Tang, Y.J. Li, A novel “turn-off” fluorescent sensor for Al^{3+} detection based on quinolinecarboxamide-coumarin, Inorg. Chem. Commun. 121 (2020) 108168.

[26] K. Zhang, H. Zheng, C.J. Hua, M. Xin, J.R. Gao, Y.J. Li, Novel fluorescent N,O-chelated fluorine-boron benzamide complexes containing thiadiazoles: Synthesis and fluorescence characteristics, Tetrahedron 74 (2018) 4161–4167.

[27] S. Sasaki, G.P.C. Drummen, G. Konishi, Recent advances in twisted intramolecular charge transfer (TICT) fluorescence and related phenomena in materials chemistry, J. Mater. Chem. C 4 (2016) 2731–2743.

[28] E.J. Gabriel, A.S. Claudia, S.G. Natalia, J.T. Juan, A.G. Carlos, M.P. Carlos, B.P. Adriana, A.V. Mariano, A.C. Carlos, A.M. Hernan, An experimental and TD-DFT theoretical study on the photophysical properties of Methylene Violet Bernthsen, Dyes Pigments 112 (2015) 341–351.

[29] S. Khemakhem, S. Elleuch, N.B. Azaza, H. Ammar, Y. Abid, Hydrolysis and substitution effects on the optical properties of coumarin derivatives studied by vibrational spectroscopy and DFT calculation, J. Mol. Struct. 1168 (2018) 65–72.

[30] E. Borkowski, F.M. Cecati, F.D. Suvire, D.M. Ruiz, C.E. Ardanaz, G.P. Romanelli, R.D. Enriz, Mass spectrometry and theoretical calculations about the loss of methyl radical from methoxilated coumarins, J. Mol. Struct. 1093 (2015) 49–58.

[31] A. Dhar, N.S. Kumar, P.K. Paul, S. Roy, R.L. Vekariya, Influence of tagging thiophene bridge unit on optical and electrochemical properties of coumarin based dyes for DSSCs with theoretical insight, Org. Electron. 53 (2018) 280–286.

[32] J. Zheng, Y.J. Li, Y.H. Cui, J.H. Jia, Q. Ye, L. Han, J.R. Gao, Isatin-phenylhydrazone dyes and boron complexes with large Stokes shifts: synthesis and solid-state fluorescence characteristics, Tetrahedron 71 (2015) 3802–3809.

[33] M.J. Frisch, G.W. Trucks, H.B. Schlegel, G.E. Scuseria, M.A. Robb, J.R. Cheeseman, V.G. Zakrzewski, J.A. Montgomery, R.E. Stratmann, J.C. Burant, S. Dapprich, J.M. Millam, A.D. Daniels, K.N. Kudin, M.C. Strain, O. Farkas, J. Tomasi, V. Barone, M. Cossi, R. Cammi, B. Mennucci, C. Pomelli, C. Adamo, S. Clifford, J. Ochterski, G.A. Petersson, P.Y. Ayala, Q. Cui, K. Morokuma, D.K. Malick, A.D. Rabuck, K. Raghavachari, J.B. Foresman, J. Cioslowski, J.V. Ortiz, B.B. Stefanov, G. Liu, A. Liashenko, P. Piskorz, I. Komaromi, R. Gomperts, R.L. Martin, D.J. Fox, T. Keith, M.A. Al-Laham, C.Y. Peng, A. Nanayakkara, C. Gonzalez, M. Challacombe, P.M.W. Gill, B.G. Johnson, W. Chen, M.W. Wong, J.L. Andres, M. Head-Gordon, E.S. Replogle, J.A. Pople, Gaussian 09, Gaussian:, Wallingford, CT, 2009.

[34] L. Vachova, V. Novakova, K. Kopecky, M. Miletina, P. Zimcik, Effect of intramolecular charge transfer on fluorescence and singlet oxygen production of phthalocyanine analogues, Dalton Trans. 41 (2012) 11651.

[35] J.Y. Lia, C.Y. Zhang, S. Wu, X. Wen, Z. Xi, L. Yi, Facile synthesis of green-light and large Stokes-shift emitting coumarins for bioconjugation, Dyes Pigments 151 (2018) 303–309.